J. Fluid Mech. (1995), *vol.* 298, *pp.* 287–309

Instability of a non-wetting film with interfacial viscous stress

By DAVID A. EDWARDS[1]† AND ALEXANDER ORON[2]

[1] Department of Chemical Engineering, Massachusetts Institute of Technology, Cambridge, MA 02139, USA

[2] Faculty of Mechanical Engineering and Center for Research in Nonlinear Phenomena, Technion-Israel Institute of Technology, Haifa, 32000 Israel

(Received 7 June 1993 and in revised form 28 February 1995)

The destabilization of a thin three-dimensional non-wetting film above a solid wall is examined for the special case in which surfactant is adsorbed onto the free surface of the film. Attention is restricted to the case of a Newtonian surface, with surfactant displaying rapid surface diffusion or exhibiting small Marangoni number, such that the dominant intrinsic interfacial stress is of a purely viscous origin. A surface-excess force approach is adopted for the purpose of incorporating into the analysis the attractive/repulsive dispersive forces acting between the solid wall and the film. Three coupled nonlinear partial differential equations are obtained that describe the 'large-wavelength' spatio-temporal evolution of the free film surface following a small initial disturbance. These equations are shown to reduce to results in the literature in the limit of zero interfacial viscosities. Employing linear stability analysis, an explicit dispersion equation is obtained relating the growth coefficient to interfacial viscosities. It is found, at least in the linear regime, that the sum of interfacial shear and dilatational viscosities – and not each separately – imparts a damping effect that in the most extreme case is four-fold relative to the case of no interfacial viscosities. Nonlinear stability analysis in the limiting case of a two-dimensional film indicates that interfacial viscosities may strongly hinder the onset of instability through large interfacial stresses that arise in the vicinity of trough and crest regions of the film.

1. Introduction

A thin liquid film at rest upon a solid surface whose physicochemical nature is such as to repulse the supported layer is found to be unstable to minuscule departures from its hydrostatic configuration. This phenomenon is commonly observed in the breakup of a thin layer of water on a waxed surface (Jain & Ruckenstein 1976; Williams & Davis 1982). If a surfactant is adsorbed to the free surface of the non-wetting film, the robustness of its equilibrium state can be enhanced to a significant degree because adsorbed surfactant may impart to the free interface intrinsic rheological properties – principally, interfacial viscosities and elasticities.

This damping role of interfacial rheological properties is illustrated in the present study, which aims to develop a set of (nonlinear) partial differential equations describing the time-evolution of a free surfactant-adsorbed fluid interface above a (three-dimensional) non-wetting thin film whose lower (solid) surface is oriented perpendicular to gravity. The analysis serves to extend the two-dimensional linear

† Present address: David A. Edwards, Department of Chemical Engineering, 204 Fenske Laboratory, Penn State University, University Park, PA 16802, USA.

stability analysis of Jain & Ruckenstein (1976), as well as the nonlinear study of Williams & Davis (1982), the latter of which does not include the effects of interfacial rheological properties.

In a companion study, Oron & Edwards (1993) have applied a weakly nonlinear stability analysis to the problem posed by a liquid film falling under gravity along a vertical plane in the presence of interfacial viscous stress. Previously, Whitaker (1964) had shown via linear stability theory that the effect of increasing interfacial viscosities is to lower the critical wavenumber, as well to suppress the wavenumber and growth rate of the most amplified mode. In their nonlinear analysis, Oron & Edwards (1993) (employing alternative scalings to those of Whitaker 1964), found that the evolution of the thin-film free surface is governed by an equation combining the well-known Kuramoto–Sivashinsky and Korteweg–de Vries equations. To the order of approximation used in their analysis, interfacial viscosities were observed *not* to necessarily have an impact on the critical and fastest growing modes. In the present study, the linear and nonlinear dynamics of the free surface of a thin non-wetting film are again found to exhibit substantially different characteristics. Whereas the linear analysis indicates a maximum damping effect of four-fold by interfacial viscous stresses, the nonlinear analysis shows that a much greater instability damping effect can occur by means of interfacial viscosities, to the extent that the growth of the film instability may be significantly arrested.

The present contribution provides a complement to several articles (Sharma & Ruckenstein 1986; Williams & Davis 1982; Burelbach, Bankoff & Davis 1988; Tan, Bankoff & Davis 1990; Jensen & Grotberg 1992) devoted to the study of the impact of long-range dispersive forces (as well as the effects of thermocapillarity, condensation/evaporation, and other physicochemical phenomena) on the nonlinear evolution of a thin liquid film. Dispersive forces have been shown in these studies potentially to induce instability of the film, possibly leading to its rupture: nonlinear interactions between dispersive forces and surface tension have been found (Sharma & Ruckenstein 1986; Williams & Davis 1982) to accelerate the film rupture.

The plan of the present paper is as follows. In §2 the hydrodynamical problem is set forth, first in dimensional, then in non-dimensional form. The long-range dispersive forces acting on the film and originating at the solid plane are included in the analysis by way of a surface-excess force assigned to the interface. This approach is described in §2 in the context of the more common *body-force* and *disjoining-pressure* approaches to thin-film hydrodynamics. A perturbation solution is obtained in §3 for large-wavelength disturbances, ultimately arriving at three nonlinear partial differential equations (cf. (3.20) to (3.22)) by which the instantaneous configuration of the interface can be studied as a function of time. In the circumstance of zero interfacial viscosities, the three partial differential equations combine to yield a single (nonlinear) kinetic equation for the interface shape, in accordance with the results of Williams & Davis (1982). In §4, a linear stability analysis is provided by which an explicit dispersion equation is derived including the effects of interfacial viscosities. In the case of infinitely large interfacial viscosities, it is shown that interfacial viscosities exhibit at most a four-fold damping effect relative to the zero interfacial viscosity case. Finally, in §5 results of a numerical analysis of the fully nonlinear equations in the case of a two-dimensional film are discussed.

2. Problem formulation

Consider a film of liquid initially at rest upon a planar solid surface whose unit normal vector $\boldsymbol{i}_3$ points in a direction parallel (and opposite) to the gravity field $\boldsymbol{g}$. A (non-ionic) surfactant A, say, is dissolved within the film and adsorbed onto its free surface at the equilibrium concentration ρ^s_{Ao}. The equilibrium surface tension σ'_o of the free surface is uniform, with a value below that of the pure (non-surfactant-adsorbed) surface. An additional effect of the adsorbed surfactant is to engender sensible interfacial shear (μ^s) and dilatational (κ^s) viscosities. Above the film is a passive air phase.

Extremely small thermally excited capillary waves exist at the free surface, as evidenced by minute fluctuations of the film thickness h' about its equilibrium height h'_o; these produce fluctuations in the surface-excess surfactant concentration ρ^s_A about its equilibrium value ρ^s_{Ao}. Moreover, owing to the concentration dependence of interfacial tension σ', simultaneous random departures of interfacial tension from its equilibrium value σ'_o occur. The magnitude of these departures is governed by the so-called *Gibbs elasticity*,

$$E_o \overset{\text{def}}{=} -\left(\frac{\partial \sigma'}{\partial \ln \rho^s_A}\right)_o, \tag{2.1}$$

where the subscript o serves (as elsewhere) to denote evaluation of the subscripted quantity at the undisturbed equilibrium state.

The equilibrium film thickness h'_o is assumed sufficiently small (100 nm, say) to show the sensible action of long-range dispersive forces over the entire thickness of the film. These forces are presumed to originate in the molecular repulsive/attractive interaction of the respective solid, fluid and air phases. The dispersive forces may either be of such a nature as to attract the (wetting) liquid film toward the solid surface or to repel the (non-wetting) film.

The thin-film stability problem arising on account of the existence of the internal repulsive/attractive film force is analogous to the classical stability problem of two immiscible liquids of different specific gravity in an external gravitational field. That is, in the case of a thin non-wetting film sandwiched between an air phase and a solid wall, the non-wetting phase plays the role of the less-dense fluid in a superposed-fluid scenario that finds the less-dense fluid beneath the heavier fluid. The intermolecular force of the non-wetting-film problem corresponds to the gravity force of the superposed-fluids problem. Both scenarios share in common the fact that any perturbation of the free surface from a plane-parallel shape necessarily draws the upper ('wetting' or 'heavier') phase towards the solid wall and therefore minimizes the total force potential acting on the system, reflecting the instability of both configurations.

The uniqueness of the present thin-film stability problem *vis-a-vis* the superposed fluid problem is that the force driving the destabilization process is wholly internal to the system. This causes some ambiguity in the hydrodynamic treatment. Since the net body force acting on the entire film system (discounting gravity) is zero, the destabilizing force may either be attributed to a body force or a contact force acting within the film. This explains why two approaches to thin-film hydrodynamical problems have been pursued in the past: in the so-called *disjoining-pressure* approach (Deryaguin & Kusakov 1937; Deryaguin 1955), internal film forces are assigned to a *contact force* termed the 'disjoining pressure', whereas in the so-called *body-force* approach (Felderhof 1968; Sche & Fijnaut 1978; Maldarelli & Jain 1982; de Gennes, Hua & Levinson 1990), internal film forces are assigned to a film-level body force.

A third alternative is pursued in the present study. The attractive/repulsive force potential is assigned to the free surface as a surface-excess body force vector density $\boldsymbol{F}^s$. This is essentially equivalent to the disjoining-pressure approach in the limiting case of a plane-parallel film (see Edwards, Brenner & Wasan 1991 for a comparison of the two approaches). In this regard, the advantage of the surface-excess force method is that it applies to arbitrarily curved fluid interfaces, whereas disjoining pressure is classically defined for plane- (or nearly plane-) parallel film configurations.

The surface-excess force $\boldsymbol{F}^s$ is assumed to derive from long-range (van der Waals) forces between solid, fluid and air molecules. For all deformations encountered in this study, $\boldsymbol{F}^s$ acts in a direction normal to the solid surface (though not necessarily normal to the free liquid surface); hence,

$$\boldsymbol{F}^s = \boldsymbol{i}_3 F^s. \tag{2.2}$$

In the case of a plane-parallel film of infinite extent, the appropriate constitutive expression for F^s is provided by (Deryaguin & Landau 1941; Verwey & Overbeek 1948)

$$F^s = -\frac{A}{6\pi h_o'^3}. \tag{2.3}$$

Here, A is the (dimensional) Hamaker constant. Microscale random fluctuations in the film thickness h_o' thus give rise to corresponding fluctuations in $\boldsymbol{F}^s$.

Note that, according to (2.2) and (2.3), when

$$A > 0,$$

the fluid surface is attracted to the solid wall. This corresponds to the case of a *non-wetting* film (i.e. for which the 'wetting' air phase is attracted to the solid wall). The inherent instability of the non-wetting film may be established in a simple, heuristic manner by inspection of the normal stress condition at the free fluid interface in hydrostatic equilibrium; namely,

$$p_o - p_a = 2H\sigma_o' + F^s.$$

Here, p_o denotes the equilibrium pressure acting within the film and p_a the air-phase pressure. The mean curvature scalar H, which is zero in the case of a planar film, possesses a positive value when the free surface is convex relative to the solid surface, and a negative value when it is concave. A small wave at the free surface will produce a diminution of capillary pressure in 'trough' regions of the film and a growth of capillary pressure in 'crest' regions of the film. Whence, film fluid may be expected to flow from 'trough' regions to 'crest' regions, enhancing the departure of the film from its equilibrium, planar shape, ultimately leading to film instability.

2.1. *Dimensional problem statement*

This subsection is devoted to a formulation of the hydrodynamic problem characterizing film motion consequent to small-scale departures from the initial equilibrium state.

Let

$$\boldsymbol{r} = \boldsymbol{i}_1 x_1 + \boldsymbol{i}_2 x_2 + \boldsymbol{i}_3 x_3 \tag{2.4}$$

denote a position vector measured from an origin situated on the solid surface. Here, $(\boldsymbol{i}_1, \boldsymbol{i}_2, \boldsymbol{i}_3)$ represent a trio of orthonormal basis vectors and (x_1, x_2, x_3) the corresponding Cartesian coordinates, bounded by

$$(-\infty \leqslant x_1 \leqslant \infty, -\infty \leqslant x_2 \leqslant \infty, 0 \leqslant x_3 \leqslant h'). \tag{2.5}$$

Motion within the film is assumed to obey the Navier–Stokes equations,

$$\rho\left(\frac{\partial \boldsymbol{v}}{\partial t}+\boldsymbol{v}\cdot\boldsymbol{\nabla}\boldsymbol{v}\right)=-\boldsymbol{\nabla}p+\mu\nabla^2\boldsymbol{v}+\rho\boldsymbol{g} \tag{2.6}$$

and the continuity condition

$$\boldsymbol{\nabla}\cdot\boldsymbol{v}=0, \tag{2.7}$$

with ρ the mass density of the film, p the fluid pressure, μ the shear viscosity,

$$\boldsymbol{g}=-\boldsymbol{i}_3 g \tag{2.8}$$

the external gravitational force (with g the gravitational constant), and

$$\boldsymbol{v}=\boldsymbol{i}_1 v_1+\boldsymbol{i}_2 v_2+\boldsymbol{i}_3 v_3 \tag{2.9}$$

the fluid velocity vector. The gradient operator $\boldsymbol{\nabla}$ is

$$\boldsymbol{\nabla}\overset{\text{def}}{=}\frac{\partial}{\partial \boldsymbol{r}}\equiv \boldsymbol{i}_1\frac{\partial}{\partial x_1}+\boldsymbol{i}_2\frac{\partial}{\partial x_2}+\boldsymbol{i}_3\frac{\partial}{\partial x_3}. \tag{2.10}$$

The instantaneous location of the free fluid interface may be described by the kinematic condition

$$\frac{\partial h'}{\partial t}+\boldsymbol{v}\cdot\boldsymbol{\nabla}h'=v_3. \tag{2.11}$$

Boundary conditions upon (2.6) and (2.7) include the no-slip condition at the planar solid surface,

$$\boldsymbol{v}=\boldsymbol{0} \quad \text{at} \quad x_3=0, \tag{2.12}$$

and the interfacial stress condition at the free fluid interface (Edwards *et al.* 1991),

$$\begin{aligned}-\boldsymbol{n}\cdot\|\boldsymbol{P}\| = {} & \boldsymbol{F}^s+2H\sigma'\boldsymbol{n}+\boldsymbol{\nabla}_s\sigma'+(\kappa^s+\mu^s)\,\boldsymbol{\nabla}_s\boldsymbol{\nabla}_s\cdot\boldsymbol{v}\\ & +2\mu^s\boldsymbol{n}(\boldsymbol{b}-2H\boldsymbol{I}_s):\boldsymbol{\nabla}_s\boldsymbol{v}+2H\boldsymbol{n}(\kappa^s+\mu^s)\,\boldsymbol{\nabla}_s\cdot\boldsymbol{v}\\ & +\mu^s\{\boldsymbol{n}\times\boldsymbol{\nabla}_s[(\boldsymbol{\nabla}_s\times\boldsymbol{v})\cdot\boldsymbol{n}]-2(\boldsymbol{b}-2H\boldsymbol{I}_s)\cdot\boldsymbol{\nabla}_s\boldsymbol{v}\cdot\boldsymbol{n}\} \quad \text{at} \quad x_3=h'.\end{aligned} \tag{2.13}$$

Here, $\boldsymbol{n}$ denotes the unit surface normal,

$$\|\boldsymbol{P}\|=\boldsymbol{P}_a(x_3-h'=0+)-\boldsymbol{P}(x_3-h'=0-) \tag{2.14}$$

the jump condition on the pressure tensor across the free surface, with

$$\boldsymbol{P}_a=-\boldsymbol{I}p_a \tag{2.15}$$

the pressure tensor in the air phase (p_a being a uniform constant), and

$$\boldsymbol{P}=-\boldsymbol{I}p+\mu(\boldsymbol{\nabla}\boldsymbol{v}+\boldsymbol{\nabla}\boldsymbol{v}^{\dagger}) \tag{2.16}$$

the pressure tensor in the film. Moreover,

$$\boldsymbol{I}=\boldsymbol{i}_1\boldsymbol{i}_1+\boldsymbol{i}_2\boldsymbol{i}_2+\boldsymbol{i}_3\boldsymbol{i}_3 \tag{2.17}$$

is the spatial idemfactor,

$$\boldsymbol{b}\overset{\text{def}}{=}-\boldsymbol{\nabla}_s\boldsymbol{n} \tag{2.18}$$

the surface curvature dyadic,

$$2H\equiv\boldsymbol{I}_s:\boldsymbol{b} \tag{2.19}$$

the mean surface curvature,

$$\boldsymbol{I}_s\overset{\text{def}}{=}\boldsymbol{I}-\boldsymbol{n}\boldsymbol{n} \tag{2.20}$$

the surface idemfactor, and

$$\nabla_s \overset{\text{def}}{=} \boldsymbol{I}_s \cdot \nabla \tag{2.21}$$

the surface gradient operator. Also, (:) denotes the double-dot operation according to the nesting convention $\boldsymbol{ab}:\boldsymbol{cd} = (\boldsymbol{a}\cdot\boldsymbol{d})(\boldsymbol{b}\cdot\boldsymbol{c})$, for any vectors $\boldsymbol{a}$, $\boldsymbol{b}$, $\boldsymbol{c}$ and $\boldsymbol{d}$.

As developed in Appendix A, the invariant differential-geometric quantities defined above may be expressed explicitly in terms of the unit vectors $(\boldsymbol{i}_1, \boldsymbol{i}_2, \boldsymbol{i}_3)$ and appropriate derivatives of the scalar function $h' \equiv h'(x_1, x_2, t)$.

The interfacial tension gradient $\nabla_s \sigma'$ appearing in (2.13) arises on account of the fact that

$$\sigma' \equiv \sigma'(\rho_A^s), \tag{2.22}$$

the explicit form of which requires an equation of state appropriate to the particular surfactant system involved. Fluctuations in the surface-excess surfactant density ρ_A^s hence manifest themselves in interfacial tension gradients $\nabla_s \sigma'$. For subsequent purposes, the equation of state may be sought in terms of a Taylor series expansion of σ' about the initial equilibrium state,

$$\sigma' = \sigma'_o + \left(\frac{\partial \sigma'}{\partial \rho_A^s}\right)_o (\rho_A^s - \rho_{Ao}^s) + \frac{1}{2!}\left(\frac{\partial^2 \sigma'}{\partial \rho_A^{s2}}\right)_o (\rho_A^s - \rho_{Ao}^s)^2 + \ldots . \tag{2.23}$$

Observe that to a linear approximation, the surface tension variation with surfactant concentration is governed *inter alia* by the Gibbs elasticity (2.1).

The surface-excess surfactant density ρ_A^s appearing in (2.23) is related to the film-phase surfactant density ρ_A by an adsorption isotherm, which here assumes the form at the free interface ($x_3 = h'$)

$$\rho_A = \rho_{Ao} + \left(\frac{\partial \rho_A}{\partial \rho_A^s}\right)_o (\rho_A^s - \rho_{Ao}^s) + \frac{1}{2!}\left(\frac{\partial^2 \rho_A}{\partial \rho_A^{s2}}\right)_o (\rho_A^s - \rho_{Ao}^s)^2 + \ldots . \tag{2.24}$$

The bulk-phase surfactant density ρ_A is assumed to obey a standard Fickian conservation law

$$\frac{\partial \rho_A}{\partial t} + \boldsymbol{v}\cdot\nabla\rho_A = D\nabla^2\rho_A, \tag{2.25}$$

subject to

$$\boldsymbol{i}_3 \cdot \nabla \rho_A = 0 \quad \text{at} \quad x_3 = 0 \tag{2.26}$$

and (Edwards *et al.* 1991)

$$\frac{\partial \rho_A^s}{\partial t} + \nabla_s \cdot (\boldsymbol{v}\rho_A^s) = D^s \nabla_s^2 \rho_A^s - D\boldsymbol{n}\cdot\nabla\rho_A \quad \text{at} \quad x_3 = h'. \tag{2.27}$$

The latter condition accounts for the accumulation and convection of surfactant in and along the free interface, as well as surface diffusion (via the interfacial diffusivity D^s) and bulk- (i.e. film-) phase diffusion to the interface. The explicit appearance of the bulk diffusivity D in (2.27) (thereby obviating the need for a kinetic adsorption relation) corresponds to our assumption of 'diffusion-controlled' surfactant transport to the interface – suggesting that the surfactant adsorption step is effectively instantaneous relative to the time required for surfactant to diffuse to the interface. This assumption typically applies to very thin films of the type considered herein.

Complete specification of the initial-boundary-value problem defined by (2.4) to (2.27) for the variables $(\boldsymbol{v}, p, h')$ requires specification of the initial disturbance values of $(\boldsymbol{v}, p, h')$ relative to their pre-initial, equilibrium values $[\boldsymbol{0}, p_o(x_3), h'_o]$.

2.2. *Non-dimensional problem statement*

Let L denote a characteristic disturbance wavelength. Inspection of (2.13) suggests the characteristic disturbance velocity U be chosen such that

$$U \equiv \epsilon^2 U_o, \tag{2.28}$$

where

$$U_o = LA/\mu h_o'^3. \tag{2.29}$$

This choice reflects the fact that macroscopic flow within the film ultimately derives from the existence of long-range attractive/repulsive forces subsumed within the surface-excess force scalar F^s. Thus, we introduce the following non-dimensionalizations:

$$\left.\begin{gathered} x_1 = xL, \quad x_2 = yL, \quad x_3 = \epsilon zL, \\ t = \tau L/U_o\epsilon^2, \quad h' = \epsilon hL, \quad p - p_a = (\mu U_o/L)\mathscr{P}, \\ v_1 = u\epsilon^2 U_o, \quad v_2 = v\epsilon^2 U_o, \quad v_3 = w\epsilon^3 U_o, \\ \rho_A = c\rho_{Ao}, \quad \rho_A^s = \Gamma^s \rho_{Ao}^s, \quad \sigma' = \sigma\sigma_o', \quad F^s = f^s A/h_o'^3. \end{gathered}\right\} \tag{2.30}$$

Next, define the following dimensionless groups:

$$\left.\begin{gathered} Ca \equiv \frac{\mu U_o}{\epsilon\sigma_o}, \quad Bo_\mu \equiv \epsilon\frac{\mu^s}{\mu L}, \quad Bo_\kappa \equiv \epsilon\frac{\kappa^s}{\mu L} \\ Re \equiv \frac{\rho U_o h_o'}{\mu}, \quad G \equiv \frac{\rho g L^2}{\epsilon^3 U_o \mu}, \quad Ad \equiv \frac{\rho_{Ao} h_o'}{\rho_{Ao}^s}, \\ Pe \equiv \epsilon\frac{U_o h_o'}{D}, \quad Pe_s \equiv \epsilon\frac{U_o h_o'}{D^s} \end{gathered}\right\} \tag{2.31}$$

respectively denoting the capillary number, the respective Boussinesq numbers, the Reynolds number, the Grashof number, the adsorption number, and the bulk and interfacial Péclet numbers. We assume in what follows that all of these dimensionless groups are $O(1)$. This is expected to be the case for a thin film whose free surface is absorbed by a dilute monolayer of surfactant. Thus, for a dilute monolayer of octanoic acid spread on a water film of 100 nm thickness above a waxed surface (Ting *et al.* 1984), $h_o' = 10^{-5}$ cm, $L = 10^{-3}$ cm, $\rho = 1$ g cm^{-3}, $\rho_{Ao} = 10^{-4}$ g cm^{-3}, $\rho_{Ao}^s = 10^{-9}$ g cm^{-2}, $\mu = 0.01$ g cm^{-1} s^{-1}, $g = 980$ cm^2 s^{-1}, $\sigma_o \sim 73$ dyne cm^{-1}, $\mu^s = \kappa^s \sim 0.01$ g s^{-1}, $D = D^s \sim 10^{-5}$ cm^2 s^{-1} and $A \sim 10^{-12}$ dyne cm. The kinematic equations subsequently developed actually have a much wider range of applicability than to dilute surfactant monolayers, as indicated in the footnote associated with (3.13).

Substitution of the dimensionless quantities (2.30) and (2.31) into (2.6)–(2.8), (2.11)–(2.16) and (2.23)–(2.27) furnishes the following dimensionless problem description:

$$\epsilon^3 Re\left[\frac{\partial u}{\partial\tau} + u\frac{\partial u}{\partial x} + v\frac{\partial u}{\partial y} + w\frac{\partial u}{\partial z}\right] = -\frac{\partial\mathscr{P}}{\partial x} + \frac{\partial^2 u}{\partial z^2} + \epsilon^2\left(\frac{\partial^2 u}{\partial x^2} + \frac{\partial^2 u}{\partial y^2}\right), \tag{2.32}$$

$$\epsilon^3 Re\left[\frac{\partial v}{\partial\tau} + u\frac{\partial v}{\partial x} + v\frac{\partial v}{\partial y} + w\frac{\partial v}{\partial z}\right] = -\frac{\partial\mathscr{P}}{\partial y} + \frac{\partial^2 v}{\partial z^2} + \epsilon^2\left(\frac{\partial^2 v}{\partial x^2} + \frac{\partial^2 v}{\partial y^2}\right), \tag{2.33}$$

$$\epsilon^5 Re\left[\frac{\partial w}{\partial\tau} + u\frac{\partial w}{\partial x} + v\frac{\partial w}{\partial y} + w\frac{\partial w}{\partial z}\right] = -\frac{\partial\mathscr{P}}{\partial z} + \epsilon^2\frac{\partial^2 w}{\partial z^2} + \epsilon^4\left(\frac{\partial^2 w}{\partial x^2} + \frac{\partial^2 w}{\partial y^2}\right) + \epsilon^4 G, \tag{2.34}$$

$$\frac{\partial u}{\partial x} + \frac{\partial v}{\partial y} + \frac{\partial w}{\partial z} = 0, \tag{2.35}$$

subject to the kinematic condition

$$\frac{\partial h}{\partial \tau}+u\frac{\partial h}{\partial x}+v\frac{\partial h}{\partial y}=w \quad \text{at} \quad z=h, \tag{2.36}$$

no-slip condition at the solid surfaces,

$$u=0, \quad v=0, \quad w=0 \quad \text{at} \quad z=0, \tag{2.37}$$

and interfacial stress boundary condition

$$\begin{aligned}
&-\boldsymbol{n}\mathscr{P}+\epsilon^2 Bo_\mu\{\boldsymbol{n}\times\bar{\boldsymbol{\nabla}}_s[(\bar{\boldsymbol{\nabla}}_s\times\bar{\boldsymbol{v}})\cdot\boldsymbol{n}]-2(\bar{\boldsymbol{b}}-2\bar{H}\boldsymbol{I}_s)\cdot\bar{\boldsymbol{\nabla}}_s\bar{\boldsymbol{v}}\cdot\boldsymbol{n}\} \quad \text{at} \quad z=h.\\
&-\boldsymbol{n}\mathscr{P}+e\boldsymbol{n}\cdot\left[(\boldsymbol{i}_x\boldsymbol{i}_z+\boldsymbol{i}_z\boldsymbol{i}_x)\frac{\partial u}{\partial z}+(\boldsymbol{i}_y\boldsymbol{i}_z+\boldsymbol{i}_z\boldsymbol{i}_y)\frac{\partial v}{\partial z}\right]\\
&\quad+\epsilon^2\boldsymbol{n}\cdot\left[2\boldsymbol{i}_x\boldsymbol{i}_x\frac{\partial u}{\partial x}+(\boldsymbol{i}_x\boldsymbol{i}_y+\boldsymbol{i}_y\boldsymbol{i}_x)\left(\frac{\partial u}{\partial y}+\frac{\partial v}{\partial x}\right)+2\boldsymbol{i}_y\boldsymbol{i}_y\frac{\partial v}{\partial y}+2\boldsymbol{i}_z\boldsymbol{i}_z\frac{\partial w}{\partial z}\right]\\
&\quad+\epsilon^3\boldsymbol{n}\cdot\left[(\boldsymbol{i}_x\boldsymbol{i}_z+\boldsymbol{i}_z\boldsymbol{i}_x)\frac{\partial w}{\partial x}+(\boldsymbol{i}_y\boldsymbol{i}_z+\boldsymbol{i}_z\boldsymbol{i}_y)\frac{\partial w}{\partial y}\right]\\
&=\boldsymbol{i}_z f^s+2\bar{H}Ca^{-1}\sigma\boldsymbol{n}+\frac{1}{\epsilon}Ca^{-1}\bar{\boldsymbol{\nabla}}_s\sigma+\epsilon(Bo_\kappa+Bo_\mu)\bar{\boldsymbol{\nabla}}_s\bar{\boldsymbol{\nabla}}_s\cdot\bar{\boldsymbol{v}}\\
&\quad+2\epsilon^2 Bo_\mu\boldsymbol{n}(\bar{\boldsymbol{b}}-2\bar{H}\boldsymbol{I}_s):\bar{\boldsymbol{\nabla}}_s\bar{\boldsymbol{v}}+2\bar{H}\epsilon^2\boldsymbol{n}(Bo_\kappa+Bo_\mu)\bar{\boldsymbol{\nabla}}_s\cdot\bar{\boldsymbol{v}}\\
&\quad+\epsilon^2 Bo_\mu\{\boldsymbol{n}\times\bar{\boldsymbol{\nabla}}_s[(\bar{\boldsymbol{\nabla}}_s\times\bar{\boldsymbol{v}})\cdot\boldsymbol{n}]-2(\bar{\boldsymbol{b}}-2\bar{H}\boldsymbol{I}_s)\cdot\bar{\boldsymbol{\nabla}}_s\bar{\boldsymbol{v}}\cdot\boldsymbol{n}\} \quad \text{at} \quad z=h.
\end{aligned} \tag{2.38}$$

In the above, we have introduced the additional dimensionless terms

$$\bar{H}=\frac{LH}{\epsilon}, \quad \bar{\boldsymbol{b}}=\frac{L\boldsymbol{b}}{\epsilon}, \quad \bar{\boldsymbol{\nabla}}_s=\boldsymbol{\nabla}_s L, \quad \bar{\boldsymbol{v}}=\frac{\boldsymbol{v}}{\epsilon^2 U_o}, \tag{2.39a–d}$$

explicit expansions of which (in the parameter ϵ) are provided in Appendix B.

Finally,

$$\sigma=1+\left(\frac{\partial\sigma}{\partial\Gamma^s}\right)_o(\Gamma^s-1)+\frac{1}{2!}\left(\frac{\partial^2\sigma}{\partial\Gamma^{s2}}\right)_o(\Gamma^s-1)^2+\ldots \tag{2.40}$$

is the dimensionless surface equation of state,

$$c=1+\left(\frac{\partial c}{\partial\Gamma^s}\right)_o(\Gamma^s-1)+\frac{1}{2!}\left(\frac{\partial^2 c}{\partial\Gamma^{s2}}\right)_o(\Gamma^s-1)^2+\ldots \quad \text{at} \quad z=h \tag{2.41}$$

the dimensionless adsorption equation, and

$$\epsilon^2 Pe\left[\frac{\partial c}{\partial\tau}+u\frac{\partial c}{\partial x}+v\frac{\partial c}{\partial y}+w\frac{\partial c}{\partial z}\right]=\epsilon^2\left(\frac{\partial^2 c}{\partial x^2}+\frac{\partial^2 c}{\partial y^2}\right)+\frac{\partial^2 c}{\partial z^2} \tag{2.42}$$

the convective–diffusion equation. The latter is subject to

$$\frac{\mathrm{d}c}{\mathrm{d}z}=0 \quad \text{at} \quad z=0, \tag{2.43}$$

and

$$\epsilon^2 Pe_s\left[\frac{\partial \Gamma^s}{\partial \tau}+\bar{\nabla}_s\cdot(\bar{v}\Gamma^s)\right]=\epsilon\bar{\nabla}_s^2\Gamma^s-Ad\frac{Pe_s}{Pe}(\boldsymbol{n}\cdot\boldsymbol{i}_z)\frac{\partial c}{\partial z}$$
$$-\epsilon Ad\frac{Pe_s}{Pe}\boldsymbol{n}\cdot\left(\boldsymbol{i}_x\frac{\partial c}{\partial x}+\boldsymbol{i}_y\frac{\partial c}{\partial y}\right)\quad\text{at}\quad z=h. \tag{2.44}$$

3. Perturbation expansion solution

A solution to the hydrodynamic problem characterized by (2.32)–(2.44) (joined by an explicit initial disturbance condition) is sought below for the condition

$$\epsilon\ll 1, \tag{3.1}$$

corresponding to the case of 'long-wavelength' film deformations, in other words where gradients parallel to the solid surface are considerably smaller than those normal to the solid.

The following power-series expansions:

$$u=u^0+\epsilon u^1+\epsilon^2u^2+\ldots,\quad v=v^0+\epsilon v^1+\epsilon^2v^2+\ldots, \tag{3.2a, b}$$
$$w=w^0+\epsilon w^1+\epsilon^2w^2+\ldots,\quad \mathscr{P}=\mathscr{P}^0+\epsilon\mathscr{P}^1+\epsilon^2\mathscr{P}^2+\ldots, \tag{3.2c, d}$$
$$f^s=f^{s0}+\epsilon f^{s1}+\epsilon^2f^{s2}+\ldots,\quad c=c^0+\epsilon c^1+\epsilon^2c^2+\ldots, \tag{3.2e, f}$$
$$\Gamma^s=\Gamma^{s0}+\epsilon\Gamma^{s1}+\epsilon^2\Gamma^{s2}+\ldots, \tag{3.2g}$$

may be substituted into (2.32)–(2.44), utilizing also the results of Appendix B; maintaining the leading-order terms in the parameter ϵ yields

$$\frac{\partial\mathscr{P}^0}{\partial x}=\frac{\partial^2u^0}{\partial z^2}, \tag{3.3}$$

$$\frac{\partial\mathscr{P}^0}{\partial y}=\frac{\partial^2v^0}{\partial z^2}, \tag{3.4}$$

$$\frac{\partial\mathscr{P}^0}{\partial z}=0, \tag{3.5}$$

and

$$\frac{\partial u^0}{\partial x}+\frac{\partial v^0}{\partial y}+\frac{\partial w^0}{\partial z}=0, \tag{3.6}$$

subject to

$$u^0=0,\quad v^0=0,\quad w^0=0\quad\text{at}\quad z=0, \tag{3.7}$$

$$-\mathscr{P}^0-f^{s0}=Ca^{-1}\frac{\partial^2h}{\partial x^2}+Ca^{-1}\frac{\partial^2h}{\partial y^2}\quad\text{at}\quad z=h, \tag{3.8}$$

$$\frac{\partial u^0}{\partial z}=(Bo_\kappa+Bo_\mu)\frac{\partial}{\partial x}\left(\frac{\partial u^0}{\partial x}+\frac{\partial v^0}{\partial y}\right)+Bo_\mu\frac{\partial}{\partial y}\left(\frac{\partial u^0}{\partial y}-\frac{\partial v^0}{\partial x}\right)\quad\text{at}\quad z=h, \tag{3.9}$$

$$\frac{\partial v^0}{\partial z}=(Bo_\kappa+Bo_\mu)\frac{\partial}{\partial y}\left(\frac{\partial u^0}{\partial x}+\frac{\partial v^0}{\partial y}\right)-Bo_\mu\frac{\partial}{\partial x}\left(\frac{\partial u^0}{\partial y}-\frac{\partial v^0}{\partial x}\right)\quad\text{at}\quad z=h, \tag{3.10}$$

$$\frac{\partial h}{\partial\tau}+u^0\frac{\partial h}{\partial x}+v^0\frac{\partial h}{\partial y}=w^0\quad\text{at}\quad z=h. \tag{3.11}$$

Also,

$$\frac{\partial^2 c^0}{\partial z^2} = 0, \tag{3.12}$$

subject to $$\frac{\partial c^0}{\partial z} = 0 \quad \text{at} \quad z = 0, \qquad \frac{\partial c^0}{\partial z} = 0 \quad \text{at} \quad z = h \tag{3.13a, b}$$

and $$c^0 = 1 + \left(\frac{\partial c}{\partial \Gamma^s}\right)_o (\Gamma^{s0} - 1) + \ldots \quad \text{at} \quad z = h. \tag{3.13c}$$

The surface-excess surfactant balance equation (2.44) can be shown to yield, with the above†

$$c^0 = 1, \quad \Gamma^{s0} = 1, \tag{3.13d, e}$$

indicating that, to leading order in ϵ, surfactant concentration gradients (and, likewise, interfacial tension gradients) do not arise. Therefore, to this order $\sigma = 1$ and the third term of the right-hand side of (2.38) vanishes.

Equations (2.3) and (2.30) combine to yield,‡

$$f^{s0} = -\frac{1}{6\pi h^3}, \tag{3.14}$$

whence (3.5) with the condition (3.8) gives

$$\mathscr{P}^0 = \frac{1}{6\pi h^3} - Ca^{-1}\nabla^2 h. \tag{3.15}$$

Substituting this expression into (3.3) and (3.4) reveals that

$$u^0 = -\left[\frac{1}{4\pi h^4}\frac{\partial h}{\partial x} + \frac{Ca^{-1}}{2}(\nabla^2 h)_x\right] z^2 + \alpha z \tag{3.16}$$

and $$v^0 = -\left[\frac{1}{4\pi h^4}\frac{\partial h}{\partial y} + \frac{Ca^{-1}}{2}(\nabla^2 h)_y\right] z^2 + \beta z, \tag{3.17}$$

where $$\alpha \equiv \alpha(x, y, \tau), \quad \beta \equiv \beta(x, y, \tau) \tag{3.18a, b}$$

are functions to be determined by requiring satisfaction of the interfacial stress boundary conditions. Use of (3.6) gives

$$w^0 = \left[-\frac{1}{12\pi}\nabla^2(h^{-3}) + \frac{Ca^{-1}}{2}\nabla^4 h\right]\frac{z^3}{3} - (\alpha_x + \beta_y)\frac{z^2}{2}, \tag{3.19}$$

† The uniformity of surface tension at the free film surface arises in the present case as a consequence of the relatively fast surface diffusion (cf. (2.44)) assumed to occur. As discussed following (2.31), this is expected to be true in the case of a dilute monolayer of surfactant. For compressed monolayers, surface diffusion will be much smaller and surface tension gradients will contribute an important, and perhaps dominant, contribution to the intrinsic interfacial stress. However, at least for surfactant systems exhibiting a critical micelle concentration (cmc), it is possible that for surfactant concentrations significantly exceeding the cmc, the Gibbs elasticity, (2.1), will tend toward zero (see Lucassen & Hansen 1966 and Ting, Wasan & Miyano 1985), so that, even in the presence of finite surface concentration gradients, Marangoni effects will be very small; explicitly, $Ma = E_o/[\mu D(\partial c/\partial \Gamma^s)_o] \ll 1$. The results of the present analysis thus apply to these cases as well.

‡ Since, for long-wavelength disturbances $\epsilon \ll 1$, the film remains nearly plane parallel, the leading-order contribution to the surface-excess force (3.14) is that provided by (2.3). The higher-order contributions to the surface-excess force will be of a more complex character whose precise form must be derived (e.g. from Lifshitz theory: see Prieve & Russel 1988) as a function of the instantaneous surface shape. See also the Hamaker approach of Maldarelli *et al.* (1980).

where condition (3.7) has also been employed. Finally, substitution of (3.16), (3.17) and (3.19) into (3.9) to (3.11) furnishes the following three equations:

$$\alpha-\frac{h_x}{2\pi h^3}-Ca^{-1}h\nabla^2 h_x = Bo_\mu h(\alpha_{yy}-\beta_{xy}) + (Bo_\kappa+Bo_\mu)\left[h^2\left(\frac{1}{12\pi}\nabla^2(h^{-3})-\frac{Ca^{-1}}{2}\nabla^4 h\right)_x + h(\alpha_{xx}+\beta_{yx})\right], \quad (3.20)$$

$$\beta-\frac{h_y}{2\pi h^3}-Ca^{-1}h\nabla^2 h_y = -Bo_\mu h(\alpha_{yx}-\beta_{xx}) + (Bo_\kappa+Bo_\mu)\left[h^2\left(\frac{1}{12\pi}\nabla^2(h^{-3})-\frac{Ca^{-1}}{2}\nabla^4 h\right)_y + h(\alpha_{xy}+\beta_{yy})\right], \quad (3.21)$$

$$h_\tau+\left(\alpha\frac{h^2}{2}\right)_x+\left(\beta\frac{h^2}{2}\right)_y-\frac{1}{12\pi}\nabla\cdot\left(\frac{\nabla h}{h}\right)-\frac{Ca^{-1}}{6}\nabla\cdot(h^3\nabla\nabla^2 h)=0. \quad (3.22)$$

Here, we have utilized the simplified notation

$$h_x\equiv\frac{\partial h}{\partial x},\quad h_y\equiv\frac{\partial h}{\partial y},\quad h_{xx}\equiv\frac{\partial^2 h}{\partial x^2},\quad \text{etc.}, \quad (3.23)$$

as well as

$$h_\tau\equiv\frac{\partial h}{\partial\tau}. \quad (3.24)$$

Equations (3.20)–(3.22) provide three coupled nonlinear differential equations by which the functions $\alpha(x,y,\tau)$, $\beta(x,y,\tau)$ and $h(x,y,\tau)$ are to be determined.

In the limiting case of zero interfacial viscosities (3.22) becomes

$$h_\tau=-\frac{1}{6\pi}\nabla\cdot\left(\frac{\nabla h}{h}\right)-\frac{Ca^{-1}}{3}\nabla\cdot[h^3\nabla(\nabla^2 h)]. \quad (3.25)$$

This result was first obtained by Williams & Davis (1982).

Equation (3.25) represents a single equation in the unknown $h(x,\tau)$, to be solved together with appropriate (e.g. periodic) boundary conditions on x and y and an initial disturbance condition. (Williams & Davis 1982 have provided a numerical study of the one-dimensional version of this equation. The evolution of an initial disturbance of the free surface is found to result in a rupture of the film which manifests itself in the emergence of spots of zero thickness h. Naturally, as the magnitude of surface tension, characterized by the inverse capillary number Ca^{-1}, increases, the growth of the disturbance is slower and the rupture time is longer.) The instability of the film, being reflected in the growth of $h(x,\tau)$ with time τ following an initial perturbation from equilibrium, is driven by the first term on the right-hand side of the equation. This, however, is only true for a non-wetting film. For a wetting film the term $-(1/6\pi)\nabla\cdot(\nabla h/h)$ changes sign – thus becoming stabilizing – since for a wetting film

$$A<0. \quad (3.26)$$

These observations follow upon noting that the characteristic velocity U_o (cf. (2.29)) reverses sign when the Hamaker constant A is negative, resulting in a sign reversal in both the capillary number Ca (cf. (2.31)) and the dimensionless time τ (cf. (2.30)). The second term on the right-hand side of (3.25) is dissipative for both wetting and non-wetting films, reflecting the stabilizing role of interfacial tension.

The set of partial differential equations (3.20)–(3.22) must be accompanied by appropriate boundary conditions. A numerical study of these equations is undertaken in §5. In the linearized calculations that follow (in §4), it will be assumed that the film consists of periodic cells, whence the boundary conditions for the film thickness $h(x,\tau)$ are themselves periodic. Periodicity of the x- and y-components of the velocity field (cf. (3.16) and (3.17)) results in periodic boundary conditions on the functions $\alpha(x,y,\tau)$ and $\beta(x,y,\tau)$.

4. Linear stability analysis

Considerable insight may be gained upon linearizing (3.20)–(3.22) around the equilibrium state, $h = h_o + \phi$, where $\phi \ll h_o$ (such that $(\alpha,\beta) \ll 1$). In this case, we obtain the trio of equations

$$\alpha - \frac{\phi_x}{2\pi h_o^3} - Ca^{-1} h_o \nabla^2 \phi_x = Bo_\mu h_o(\alpha_{yy} - \beta_{xy}) + (Bo_\kappa + Bo_\mu)\left[-\frac{1}{4\pi h_o^2}\nabla^2\phi_x - \frac{Ca^{-1}}{2} h_o^2 \nabla^4 \phi_x + h_o(\alpha_{xx} + \beta_{yx})\right], \quad (4.1)$$

$$\beta - \frac{\phi_y}{2\pi h_o^3} - Ca^{-1} h_o \nabla^2 \phi_y = -Bo_\mu h_o(\alpha_{yx} - \beta_{xx}) + (Bo_\kappa + Bo_\mu)\left[-\frac{1}{4\pi h_o^2}\nabla^2\phi_y - \frac{Ca^{-1}}{2} h_o^2 \nabla^4 \phi_y + h_o(\alpha_{xy} + \beta_{yy})\right], \quad (4.2)$$

$$\phi_\tau + \frac{h_o^2}{2}\alpha_x + \frac{h_o^2}{2}\beta_y - \frac{1}{12\pi h_o}\nabla^2\phi - \frac{Ca^{-1}}{6} h_o^3 \nabla^4 \phi = 0. \quad (4.3)$$

Substituting into these equations the waveforms $(\alpha, \beta, \phi) \propto \exp(ik_x x + ik_y y + \omega\tau)$ and imposing the existence requirement that the determinant of the coefficient matrix be zero, results in the determinant equation

$$\begin{vmatrix} \omega + \dfrac{k^2}{12\pi h_o} - \dfrac{Ca^{-1}}{6} h_o^3 k^4 & \dfrac{ik_x h_o^2}{2} & \dfrac{ik_y h_o^2}{2} \\ -ik_x q & 1 + Bo_\mu h_o k_y^2 + (Bo_\kappa + Bo_\mu) h_o k_x^2 & Bo_\kappa h_o k_x k_y \\ -ik_y q & Bo_\kappa h_o k_x k_y & 1 + Bo_\mu h_o k_x^2 + (Bo_\kappa + Bo_\mu) h_o k_y^2 \end{vmatrix} = 0, \quad (4.4)$$

where

$$q = \frac{1}{2\pi h_o^3} - Ca^{-1} h_o k^2 + (Bo_\kappa + Bo_\mu)\left(\frac{k^2}{4\pi h_o^2} - \frac{Ca^{-1}}{2} h_o^2 k^4\right) \quad (4.5)$$

and $k^2 = k_x^2 + k_y^2$.

An explicit dispersion relation $\omega \equiv \omega(k_x, k_y)$ follows upon evaluating the above determinant. This may ultimately be expressed in the form

$$\omega = \frac{k^2}{24\pi h_o}(1 - 2\pi Ca^{-1} h_o^4 k^2)\left[\frac{4 + h_o k^2 (Bo_\kappa + Bo_\mu)}{1 + h_o k^2 (Bo_\kappa + Bo_\mu)}\right]. \quad (4.6)$$

In the limit of zero interfacial viscosities ($Bo_\kappa = Bo_\mu = 0$), we find

$$\omega = \frac{k^2}{6\pi h_o}(1 - 2\pi\, Ca^{-1} h_o^4 k^2), \quad (4.7)$$

whence for small wavelengths ($k \gg 1$) (this limit, as further discussed below, is not strictly valid given the restriction (3.1)),

$$\omega \approx -\tfrac{1}{3} Ca^{-1} h_0^3 k^4$$

revealing that the interface is stable, and for large wavelengths ($k \ll 1$),

$$\omega \approx \frac{k^2}{6\pi h_0}$$

showing the interface to be unstable.

Equation (4.6) demonstrates that interfacial viscous stress cannot alter the stability properties of the modes, rather only the growth rate of the perturbations. This equation is in agreement with that derived by Ruckenstein & Jain (1974) (cf. their equation (39)) in the long-wave ($k \ll 1$) limit, representing the limit of validity of our analysis. For finite values of k their equation differs from our own owing to the approximation (3.1) made in the present analysis.

For finite interfacial viscosities, we have the seemingly remarkable fact that the interfacial shear and dilatational viscosities do not appear independently in (4.6). While this observation also applies to the two-dimensional linear stability analysis of Jain & Ruckenstein (1976), it is indeed a requirement of 'one-dimensional' interfacial rheological problems involving Newtonian interfaces that interfacial shear and dilatational viscosities act as a single viscous property of the interface. This may be seen from the limiting form which the interfacial stress equation (2.18) obtains for a one-dimensional interface, namely,

$$-\boldsymbol{n}\cdot\|\boldsymbol{P}\| = \boldsymbol{F}^s + 2H\sigma'\boldsymbol{n} + \boldsymbol{\nabla}_s\sigma' + (\kappa^s+\mu^s)\,\boldsymbol{\nabla}_s\boldsymbol{\nabla}_s\cdot\boldsymbol{v} + 2H\boldsymbol{n}(\kappa^s+\mu^s)\,\boldsymbol{\nabla}_s\cdot\boldsymbol{v} \quad \text{at} \quad x_3 = h', \tag{4.8}$$

which result underlies the Cartesian-component interfacial stress equation employed by Oron & Edwards (1993). However, there seems to be no *a priori* reason to have suspected the same to be true in the three-dimensional (two-dimensional interface) case, and it is expected that for the full nonlinear treatment of the problem (as embodied in (3.20)–(3.22)) this combined manifestation of interfacial shear and dilatational viscous effects will not occur.

In the limit of infinite Boussinesq numbers, (4.6) gives

$$\omega = \frac{k^2}{24\pi h_0}(1 - 2\pi\, Ca^{-1} h_0^4 k^2), \tag{4.9}$$

revealing (upon comparison with (4.7)) that interfacial viscosities have at most a four-fold damping effect. This conclusion was first reached by Jain & Ruckenstein (1976) in their two-dimensional (one-dimensional interface) investigation of this same problem.

In figure 1 neutral stability curves $\omega = \omega(k)$ of the dispersion relation (4.6) are shown for the cases of $B = 0, 1, 10, 100$ (where $B = Bo_\mu + Bo_\kappa$) when $Ca = 1$ (with also $h_0 = 1$). For a fixed value of Ca, the growth rate ω of perturbations may be observed to decrease with increasing interfacial viscosities (i.e. B), thus the growth rate is highest when interfacial viscosities are absent ($B = 0$). (It may also be shown that, for a given value of B, the lower is the capillary number Ca, the narrower is the range of linearly unstable modes corresponding to $\omega > 0$.) Variation of B does not affect the band of unstable modes $0 < k < k_0$ and the dominant wavenumber, k_M (obtained from (4.6) by setting $\partial\omega/\partial k = 0$), possesses the value

$$k_M = \frac{1}{2h_0^2(\pi\, Ca^{-1})^{1/2}} \tag{4.10}$$

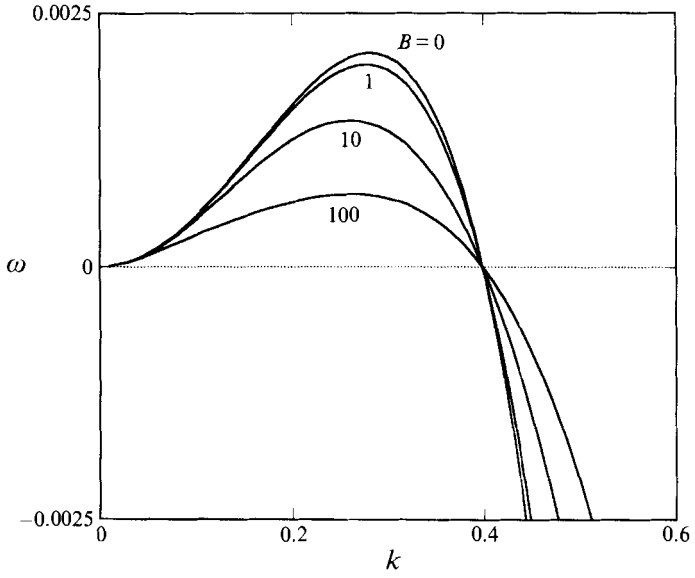

FIGURE 1. Growth coefficient ω versus wavenumber k at various values of the Boussinesq number sum $B = Bo_\mu + Bo_\kappa$ and at fixed capillary number $Ca = 1$. The results are based upon (4.6) with an equilibrium dimensionless film thickness $h_0 = 1$.

for both the cases of zero ($B \to 0$) and infinite ($B \to \infty$) interfacial viscosities, only slightly deviating from this value for finite interfacial viscosities. The above result is in agreement with that obtained by Jain & Ruckenstein (1976).

5. Nonlinear stability analysis

We limit our numerical investigation of the strongly nonlinear regime to the two-dimensional case, independent of y. Equations (3.20)–(3.22) reduce to

$$h_\tau + \tfrac{1}{2}(\alpha h^2)_x - \frac{1}{12\pi}\left(\frac{h_x}{h}\right)_x - \frac{Ca^{-1}}{6}(h^3 h_{xxx})_x = 0, \tag{5.1}$$

$$Bh\alpha_{xx} - \alpha = -\frac{h_x}{2\pi h^3} - Ca^{-1} h h_{xxx} - Bh^2\left(\left(\frac{h^{-3}}{12\pi}\right)_x - \frac{Ca^{-1}}{2} h_{xxx}\right)_{xx}, \tag{5.2}$$

where $B = Bo_\kappa + Bo_\mu$ and $\alpha = \alpha(x, \tau)$. Equations (5.1) and (5.2) are to be supplemented by periodic boundary conditions for α and h in the domain $0 \leqslant x \leqslant L$, and an initial condition $h(x, 0) = h_0(x)$ of the following two types:

$$h_0(x) = 1 + \delta \sin(k_0 x), \quad h_0(x) = 1 + \delta r(x), \tag{5.3a, b}$$

where $\delta \ll 1$ is a constant, $r(x)$ is a random function uniformly distributed in the interval $(-1, 1)$ and k_0 is the fundamental mode that can be accommodated in the domain. Equations (5.1) and (5.2) are numerically solved using the following procedure: first, (5.2) is solved to find α employing $h(x, \tau)$ determined previously for a given τ or specified in the initial condition; next, the function α calculated from the previous step is introduced into (5.1) to calculate $h(x, \tau + \delta\tau)$, where $\delta\tau$ is a small time step. The procedure is then repeated to compute $h(x, \tau)$ at the next time level.

Tens of numerical experiments were performed with (5.1) and (5.2) in order to follow the spatio-temporal evolution of the film for different values of the parameters in the

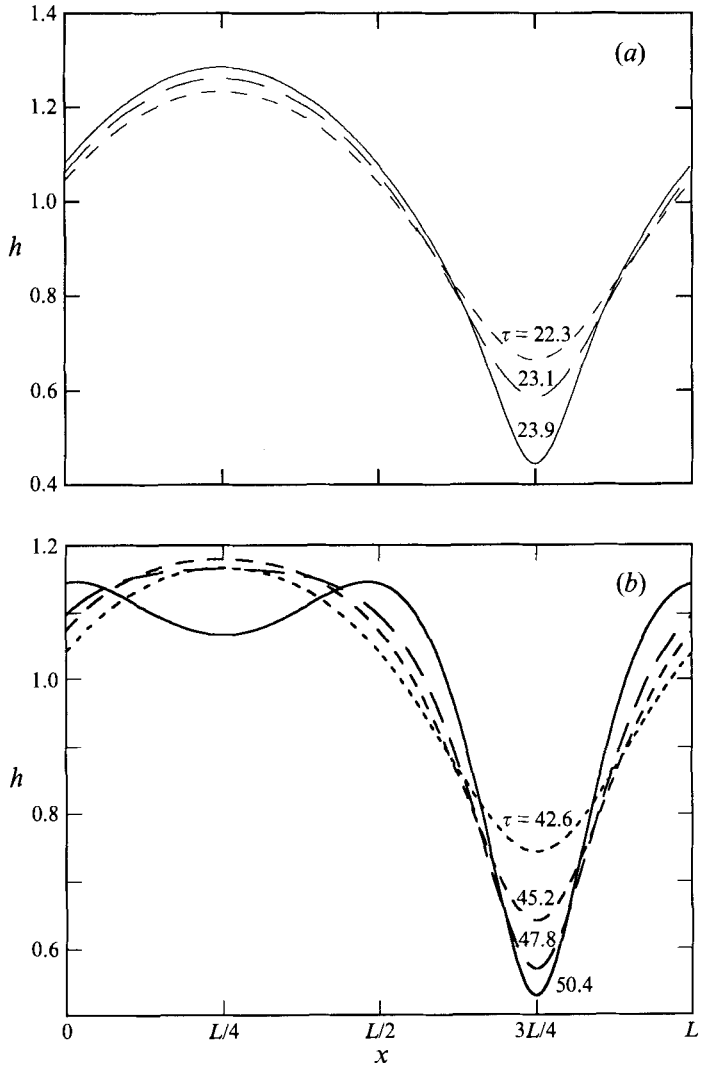

FIGURE 2. Spatio-temporal evolution of the film interface as described by (5.1) and (5.2) for $Ca^{-1} = 0.01$, $L = 2.5133$ ($k_o = 2.5$). The initial condition is $h_0 = 1 + 0.01 \sin(k_0 x)$. The fastest growing mode for the given values of the parameters is $k_M = 2.821$. (*a*) $B = 0.1$; the curves correspond to the times $\tau = 22.3$, 23.1, and 23.9. The curve corresponding to $\tau = 23.9$ represents the state topologically similar to the steady solution for (5.1) and (5.2). (*b*) $B = 1.0$; the curves correspond to the times, $\tau = 42.6$, 45.2, 47.8, and 50.4. The curve corresponding to $\tau = 50.4$ represents the state topologically similar to the steady solution for (5.1) and (5.2). Diminution of the rate of film rupture is clearly seen.

ranges $0.01 \leqslant Ca^{-1} \leqslant 1$ and $0.05 \leqslant B \leqslant 5$. The domain size L was chosen in the range $0.5\lambda_M \leqslant L \leqslant 10\lambda_M$, where λ_M is the fastest wavelength based on linear stability, as given by (4.10), $\lambda_M = 2\pi/k_M \approx 4\pi h_0^2(\pi Ca^{-1})^{1/2}$. In all the cases studied, the evolution of the initial data given either by (5.3*a*) or (5.3*b*) leads to a diminution of the rate of the film rupture process and to the emergence of steady solutions of (5.1) and (5.2).

Figures 2(*a*) and 2(*b*) display typical examples of the spatio-temporal evolution of the film starting with the initial data (5.3*a*) with $\delta = 0.01$, $Ca^{-1} = 0.01$ and for $B = 0.1$ and 1, respectively. The domain size L in these examples is larger than λ_M. In the case

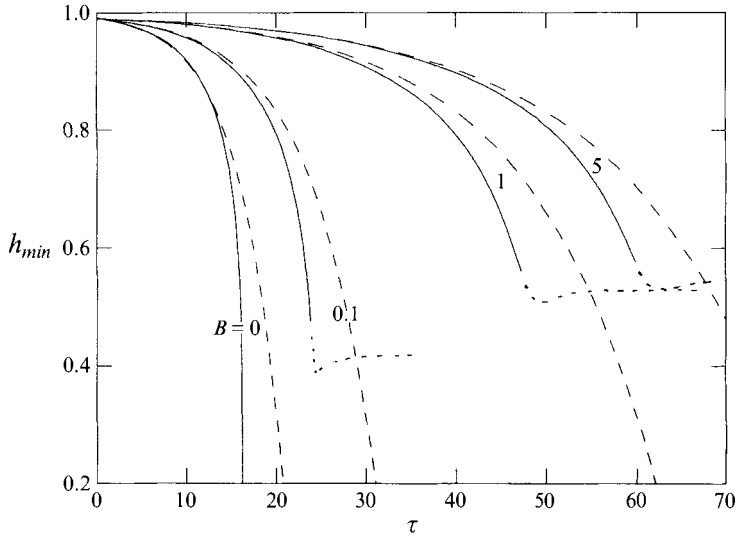

FIGURE 3. Temporal evolution of the minimum film thickness h_{min} for $Ca^{-1} = 0.01$, $L = 2.5133$ ($k_0 = 2.5$) and for various values of B. The initial condition is $h_0 = 1 + 0.01 \sin(k_0 x)$. Solid curves represent the nonlinear evolution as found from the solution of (5.1) and (5.2), while the corresponding dashed curves represent the linear evolution in accordance with (4.6), with $k = k_M$. The dotted curves represent the stage of the evolution that is formally beyond the validity of the long-wave theory.

of a small Boussinesq number B, e.g. $B = 0.1$, the crest flattens out during the evolution while remaining convex. For higher values of B, e.g. $B = 1$, the crest splits into two secondary crests. The appearance of the secondary wave at the higher Boussinesq number is attributed to the ability of the interface to intrinsically resist (via sensible interfacial viscosities) deformation of the interface caused by the van der Waal attraction of the interface toward the lower surface. In the deepest trough shown in figure 2(*b*), a large interfacial viscous stress accompanies the relatively large local surface curvature. This stress is effectively distributed across the entire free surface by the appearance of the secondary trough, which enhances the intrinsic interfacial resistance of the interface by inducing surface curvature.

The time evolution of the minimum film thickness is presented in figure 3 for various values of B (solid curves) along with the evolution predicted by the linear theory (cf. (4.6)), corresponding to $k = k_M$ and $Ca^{-1} = 0.01$ (dashed curves). The curve corresponding to a pure interface with no interfacial viscosities, $B = 0$, represents the result of Williams & Davis (1982). As predicted, the film ruptures under the influence of the van der Waals forces. In the presence of interfacial viscous stress, the perturbation grows and saturates at the thickness $h = h^o_{min}$. The minimum thickness h^o_{min} increases with increasing B when Ca and L are fixed. Comparison of the curves corresponding to the linear and nonlinear evolutions shows that three different stages exist. First, the perturbation grows in accordance with the linear theory. Next, the disjoining pressure dominates and the growth rate of the perturbation is superlinear. Finally, the growth is dominated by interfacial viscous stress, resulting in strong damping of the rate of film thinning and, ultimately, saturation of the disturbance (i.e. the dotted segments of the curves).

The saturation of the film disturbance, corresponding to $h = h^o_{min}$, is a very surprising result. It appears to indicate that the effect of finite interfacial viscosities is

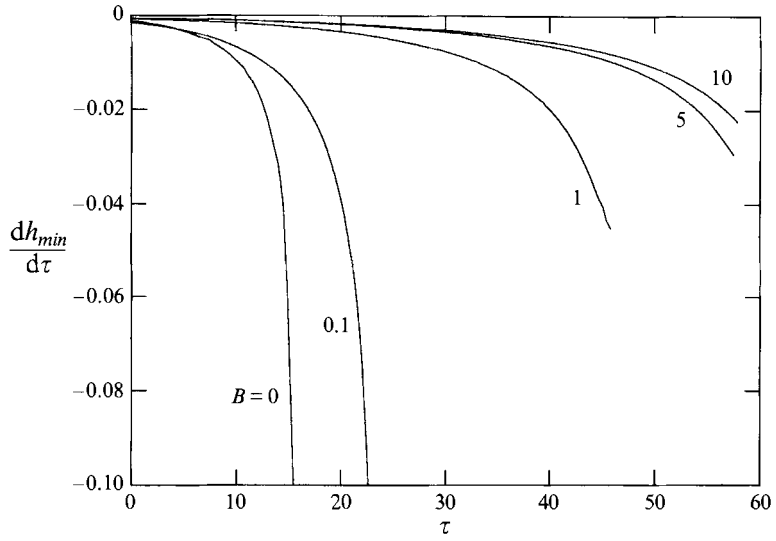

FIGURE 4. Rate of change ($dh_{min}/d\tau$) of the film thickness in the vicinity of the minimum film thickness h_{min} for $Ca^{-1} = 0.01$, $L = 2.5133$ ($k_0 = 2.5$) and for various values of B. The initial condition is $h_0 = 1 + 0.01 \sin(k_0 x)$. The curves represent the nonlinear evolution as found from the solution of (5.1) and (5.2).

to stabilize an otherwise thermodynamically unstable film. Especially surprising is the fact that the steady-state solution $h = h^o_{min}$ is accompanied by a small though finite fluid motion. This is obviously a violation of energy conservation since, in the absence of an evolving film shape, no energy is provided to the film by which this motion can be maintained. However, closer examination of the numerical results shows that prior to the attainment of the saturated solution $h = h^o_{min}$, a very large surface curvature (i.e. $h_{xx} \gg 1$) arises in the vicinity of the minimum film thickness; since the surface derivatives of h are assumed to be everywhere of order unity, this attainment of large curvature violates a basic assumption of the long-wave analysis (cf. (3.1)). Hence, the steady solutions associated with $h = h^o_{min}$ lie outside the domain of validity of (5.1) and (5.2). (Other circumstances where long-wave nonlinear stability theory is violated have recently been discussed by Salamon, Armstrong & Brown 1994.)

The emergence of steady solutions (figure 3), and particularly the disturbance damping that precedes these steady solutions, does, however, illustrate an important physical interfacial phenomenon. As the disturbance grows on the free surface of the non-wetting film, deep troughs form (figure 2). In the vicinity of these troughs, the local curvature radius becomes very small. The consequence of finite interfacial viscosities is that extremely large interfacial stresses (characterized by the local Boussinesq number $(\mu^s + \kappa^s)/\mu a$, with a the local curvature radius) arise in the trough regions, practically rendering the interface in these regions 'solid-like'. This is essentially the same phenomenon attested to by observations (Silvey 1916) early in the century that very small droplets appear to settle as solid spheres, leading Boussinesq (1913) to develop the first hydrodynamical theory of interfacial viscosity. Thus, while the steady-state solutions predicted by (5.1) and (5.2) are non-physical and lie outside the domain of validity of the analysis, the prediction of a rapid diminution of the rate of film instability, caused by interfacial viscosities, is both within the domain of mathematical validity of the theory and physically realistic. This fact is confirmed in figure 4, which displays the behaviour of the time derivative $dh_{min}/d\tau$ versus time at various values of

the Boussinesq number. The results shown lie within the domain of validity of the long-wave theory. This figure shows that, even within the 'small-curvature' conditions of the long-wave limit, the damping effect caused by interfacial viscosities is much larger than the maximum four-fold damping effect predicted by the linear theory.

We expect that a numerical analysis of the full (large-amplitude disturbance) nonlinear instability problem will show that a non-wetting film upon a solid surface progresses toward breakup relatively slowly for finite interfacial viscosities, though at a positive rate. Such an analysis should be pursued, not only for the present non-wetting film problem, but also for many other film instability problems, such as those involving coalescing bubbles and droplets. It is hoped that analyses of this type will provide theoretical insight into the body of published data (Edwards *et al.* 1991) that show interfacial viscosities and elasticities often to be controlling parameters in the stability of foam and emulsion systems.

Finally, we expect similar results as those obtained here for interfacial viscosities to apply for interfacial 'Marangoni' elasticities, insofar as the latter also lead to a 'hardening' of the interface. Of course, the occurrence of Marangoni stresses potentially introduces many other complexities into the analysis that have been avoided here, such as the precise nature of surfactant absorption/desorption kinetics and the equation of state by which interfacial tension gradients are related to the surface-excess surfactant concentration profile.

6. Summary

A nonlinear stability analysis has been presented for the case of a thin film on a non-wetting surface. By focusing attention upon the special case of either rapid surface diffusion or small Marangoni number, the role of interfacial viscosities in the damping of interfacial instabilities has been examined independently of the role of interfacial tension gradients. Three coupled nonlinear partial differential equations have been derived in the long-wavelength limit to describe the temporal evolution of the film. Linear stability analysis has shown that interfacial viscosities can cause as much as a four-fold damping of film instability. In the nonlinear regime, the interfacial viscosities give rise to a very strong film instability damping, much stronger than that predicted by the linear theory. It is important in future studies to numerically examine the evolution of large-amplitude disturbances of inherently unstable films with finite interfacial viscosities in order to clarify the degree of perturbation slowdown that can be caused by interfacial viscosities when the film surface becomes highly deformed.

A.O. acknowledges the support of the Technion V.P.R. Fund.

Appendix A. General component representations of surface invariants

In terms of the space-fixed Cartesian coordinates (x_1, x_2, x_3), the unit normal $\boldsymbol{n}$ of the surface characterized by (2.12) is

$$\boldsymbol{n} = \frac{\nabla F}{|\nabla F|} \equiv (\boldsymbol{i}_3 - \boldsymbol{i}_1 h_1' - \boldsymbol{i}_2 h_2')\, N, \tag{A 1}$$

where

$$N \overset{\text{def}}{=} \frac{1}{(1 + h_1'^2 + h_2'^2)^{1/2}}, \tag{A 2}$$

following a similar notation as in (3.23): the subscripts 1, 2 denote respectively the derivatives with respect to x_1 and x_2.

Employ (2.20) to obtain for the surface idemfactor

$$\begin{aligned}\boldsymbol{I}_s = {} & \boldsymbol{i}_1\boldsymbol{i}_1(1-N^2h_1'^2)+\boldsymbol{i}_2\boldsymbol{i}_2(1-N^2h_2'^2)+\boldsymbol{i}_3\boldsymbol{i}_3(1-N^2)\\ & +(\boldsymbol{i}_1\boldsymbol{i}_3+\boldsymbol{i}_3\boldsymbol{i}_1)N^2h_1'+(\boldsymbol{i}_2\boldsymbol{i}_3+\boldsymbol{i}_3\boldsymbol{i}_2)N^2h_2'-(\boldsymbol{i}_1\boldsymbol{i}_2+\boldsymbol{i}_2\boldsymbol{i}_1)h_1'h_2'N^2. \quad \text{(A 3)}\end{aligned}$$

Dot multiplication of (A 1) and (A 3) shows that $\boldsymbol{n}\cdot\boldsymbol{I}_s = \boldsymbol{0}$.

Use of (2.21) with the preceding results gives

$$\begin{aligned}\boldsymbol{\nabla}_s = {} & \boldsymbol{i}_1\left[(1-N^2h_1'^2)\frac{\partial}{\partial x_1}+N^2h_1'\frac{\partial}{\partial x_3}-N^2h_1'h_2'\frac{\partial}{\partial x_2}\right]\\ & +\boldsymbol{i}_2\left[(1-N^2h_2'^2)\frac{\partial}{\partial x_2}+N^2h_2'\frac{\partial}{\partial x_3}-N^2h_1'h_2'\frac{\partial}{\partial x_1}\right]\\ & +\boldsymbol{i}_3\left[(1-N^2)\frac{\partial}{\partial x_3}+N^2h_1'\frac{\partial}{\partial x_1}+N^2h_2'\frac{\partial}{\partial x_2}\right], \quad \text{(A 4)}\end{aligned}$$

whence the curvature dyadic (2.18) becomes

$$\begin{aligned}\boldsymbol{b} = {} & \boldsymbol{i}_1\boldsymbol{i}_1[(1-N^2h_1'^2)(Nh_1')_1-N^2h_1'h_2'(Nh_1')_2]\\ & +\boldsymbol{i}_2\boldsymbol{i}_2[(1-N^2h_2'^2)(Nh_2')_2-N^2h_1'h_2'(Nh_2')_1]\\ & -\boldsymbol{i}_3\boldsymbol{i}_3[N^2h_1'N_1+N^2h_2'N_2]\\ & +\boldsymbol{i}_1\boldsymbol{i}_2[(1-N^2h_1'^2)(Nh_2')_1-N^2h_1'h_2'(Nh_2')_2]\\ & +\boldsymbol{i}_2\boldsymbol{i}_1[(1-N^2h_2'^2)(Nh_1')_2-N^2h_1'h_2'(Nh_1')_1]\\ & -\boldsymbol{i}_1\boldsymbol{i}_3[(1-N^2h_1'^2)N_1-N^2h_1'h_2'N_2]\\ & +\boldsymbol{i}_3\boldsymbol{i}_1[N^2h_1'(Nh_1')_1+N^2h_2'(Nh_1')_2]\\ & -\boldsymbol{i}_2\boldsymbol{i}_3[(1-N^2h_2'^2)N_2-N^2h_1'h_2'N_1]\\ & +\boldsymbol{i}_3\boldsymbol{i}_2[N^2h_1'(Nh_2')_1+N^2h_2'(Nh_2')_2]. \quad \text{(A 5)}\end{aligned}$$

Appendix B. Explicit expansions of surface invariants

Employing the non-dimensionalized coordinates (cf. (2.30)), equations (A 2) and (A 3) allow the following perturbation expansion of the unit surface normal:

$$\boldsymbol{n} = \boldsymbol{i}_z[1-\tfrac{1}{2}\epsilon^2(h_x^2+h_y^2)]-\boldsymbol{i}_x\epsilon h_x-\boldsymbol{i}_y\epsilon h_y+O(\epsilon^3). \quad \text{(B 1)}$$

This satisfies

$$\boldsymbol{n}\cdot\boldsymbol{n} = 1+O(\epsilon^3),$$

as required. Similarly, (A 5) may be expanded in ϵ to give

$$\begin{aligned}\boldsymbol{I}_s = {} & \boldsymbol{i}_x\boldsymbol{i}_x(1-\epsilon^2h_x^2)+\boldsymbol{i}_y\boldsymbol{i}_y(1-\epsilon^2h_y^2)\\ & +\boldsymbol{i}_z\boldsymbol{i}_z\epsilon^2(h_x^2+h_y^2)+(\boldsymbol{i}_x\boldsymbol{i}_z+\boldsymbol{i}_z\boldsymbol{i}_x)\epsilon h_x\\ & +(\boldsymbol{i}_y\boldsymbol{i}_z+\boldsymbol{i}_z\boldsymbol{i}_y)\epsilon h_y-(\boldsymbol{i}_x\boldsymbol{i}_y+\boldsymbol{i}_y\boldsymbol{i}_x)\epsilon^2h_xh_y+O(\epsilon^3), \quad \text{(B 2)}\end{aligned}$$

which necessarily satisfies

$$\boldsymbol{I}_s:\boldsymbol{I}_s = 2+O(\epsilon^3)$$

and $$\boldsymbol{n}\cdot\boldsymbol{I}_s = O(\epsilon^3).$$

From (A 4) (employing the non-dimensionalization (2.39)), we have

$$\begin{aligned}\bar{\nabla}_s = \boldsymbol{i}_x&\left[(1-\epsilon^2 h_x^2)\frac{\partial}{\partial x}+\epsilon h_x\frac{\partial}{\partial z}-\epsilon^2 h_x h_y\frac{\partial}{\partial y}\right]\\ +\boldsymbol{i}_y&\left[(1-\epsilon^2 h_y^2)\frac{\partial}{\partial y}+\epsilon h_y\frac{\partial}{\partial z}-\epsilon^2 h_x h_y\frac{\partial}{\partial x}\right]\\ +\boldsymbol{i}_z&\left[\epsilon h_x\frac{\partial}{\partial x}+\epsilon h_y\frac{\partial}{\partial y}+\epsilon^2(h_x^2+h_y^2)\frac{\partial}{\partial z}\right]+O(\epsilon^3).\end{aligned} \tag{B 3}$$

The curvature dyadic $\boldsymbol{b}$ follows from (A 5) (with also (2.39)), whence

$$\begin{aligned}\bar{\boldsymbol{b}} = {}&\boldsymbol{i}_x\boldsymbol{i}_x h_{xx}+\boldsymbol{i}_y\boldsymbol{i}_y h_{yy}+(\boldsymbol{i}_x\boldsymbol{i}_y+\boldsymbol{i}_y\boldsymbol{i}_x)h_{xy}\\ &+(\boldsymbol{i}_x\boldsymbol{i}_z+\boldsymbol{i}_z\boldsymbol{i}_x)\epsilon(h_x h_{xx}+h_y h_{xy})\\ &+(\boldsymbol{i}_y\boldsymbol{i}_z+\boldsymbol{i}_z\boldsymbol{i}_y)\epsilon(h_y h_{yy}+h_x h_{yx})+O(\epsilon^2).\end{aligned} \tag{B 4}$$

This satisfies the necessary condition

$$\bar{\boldsymbol{b}} = \bar{\boldsymbol{b}}^{\dagger}.$$

Employ (2.19) and (2.39) with (B 2) and (B 4) to obtain

$$2\bar{H} = h_{xx}+h_{yy}+O(\epsilon^2) \tag{B 5}$$

for the mean surface curvature.

The following differential invariants are obtained from the above:

$$\begin{aligned}\bar{\nabla}_s\bar{\boldsymbol{v}} = {}&\boldsymbol{i}_x\boldsymbol{i}_x\left[(1-\epsilon^2 h_x^2)\frac{\partial\bar{v}_x}{\partial x}+\epsilon h_x\frac{\partial\bar{v}_x}{\partial z}-\epsilon^2 h_x h_y\frac{\partial\bar{v}_x}{\partial y}\right]\\ &+\boldsymbol{i}_x\boldsymbol{i}_y\left[(1-\epsilon^2 h_x^2)\frac{\partial\bar{v}_y}{\partial x}+\epsilon h_x\frac{\partial\bar{v}_y}{\partial z}-\epsilon^2 h_x h_y\frac{\partial\bar{v}_y}{\partial y}\right]\\ &+\boldsymbol{i}_x\boldsymbol{i}_z\left[(1-\epsilon^2 h_x^2)\frac{\partial\bar{v}_z}{\partial x}+\epsilon h_x\frac{\partial\bar{v}_z}{\partial z}-\epsilon^2 h_x h_y\frac{\partial\bar{v}_z}{\partial y}\right]\\ &+\boldsymbol{i}_y\boldsymbol{i}_x\left[(1-\epsilon^2 h_y^2)\frac{\partial\bar{v}_x}{\partial y}+\epsilon h_y\frac{\partial\bar{v}_x}{\partial z}-\epsilon^2 h_x h_y\frac{\partial\bar{v}_x}{\partial x}\right]\\ &+\boldsymbol{i}_y\boldsymbol{i}_y\left[(1-\epsilon^2 h_y^2)\frac{\partial\bar{v}_y}{\partial y}+\epsilon h_y\frac{\partial\bar{v}_y}{\partial z}-\epsilon^2 h_x h_y\frac{\partial\bar{v}_y}{\partial x}\right]\\ &+\boldsymbol{i}_y\boldsymbol{i}_z\left[(1-\epsilon^2 h_y^2)\frac{\partial\bar{v}_z}{\partial y}+\epsilon h_y\frac{\partial\bar{v}_z}{\partial z}-\epsilon^2 h_x h_y\frac{\partial\bar{v}_z}{\partial x}\right]\\ &+\boldsymbol{i}_z\boldsymbol{i}_x\left[\epsilon h_x\frac{\partial\bar{v}_x}{\partial x}+\epsilon h_y\frac{\partial\bar{v}_x}{\partial y}+\epsilon^2(h_x^2+h_y^2)\frac{\partial\bar{v}_x}{\partial z}\right]\\ &+\boldsymbol{i}_z\boldsymbol{i}_y\left[\epsilon h_x\frac{\partial\bar{v}_y}{\partial x}+\epsilon h_y\frac{\partial\bar{v}_y}{\partial y}+\epsilon^2(h_x^2+h_y^2)\frac{\partial\bar{v}_y}{\partial z}\right]\\ &+\boldsymbol{i}_z\boldsymbol{i}_z\left[\epsilon h_x\frac{\partial\bar{v}_z}{\partial x}+\epsilon h_y\frac{\partial\bar{v}_z}{\partial y}+\epsilon^2(h_x^2+h_y^2)\frac{\partial\bar{v}_z}{\partial z}\right]+O(\epsilon^3),\end{aligned} \tag{B 6}$$

whence

$$\bar{\nabla}_s\cdot\bar{v}=\frac{\partial\bar{v}_x}{\partial x}+\frac{\partial\bar{v}_y}{\partial y}+\epsilon h_y h_x\left(\frac{1}{h_y}\frac{\partial\bar{v}_x}{\partial z}+\frac{1}{h_x}\frac{\partial\bar{v}_y}{\partial z}+\frac{1}{h_y}\frac{\partial\bar{v}_z}{\partial x}+\frac{1}{h_x}\frac{\partial\bar{v}_z}{\partial y}\right)$$
$$-\epsilon^2h_x^2h_y^2\left[\frac{1}{h_y^2}\frac{\partial\bar{v}_x}{\partial x}+\frac{1}{h_xh_y}\frac{\partial\bar{v}_x}{\partial y}+\frac{1}{h_x^2}\frac{\partial\bar{v}_y}{\partial y}+\frac{1}{h_xh_y}\frac{\partial\bar{v}_y}{\partial x}\right.$$
$$\left.-\left(\frac{1}{h_x^2}+\frac{1}{h_y^2}\right)\frac{\partial\bar{v}_z}{\partial z}\right]+O(\epsilon^3) \tag{B 7}$$

and

$$\bar{\nabla}_s(\bar{\nabla}_s\cdot\bar{v})=i_x\left\{(1-\epsilon^2h_x^2)\frac{\partial}{\partial x}\left(\frac{\partial\bar{v}_x}{\partial x}+\frac{\partial\bar{v}_y}{\partial y}\right)+\left(\epsilon\frac{\partial}{\partial x}+\epsilon^2h_x\frac{\partial}{\partial z}\right)\right.$$
$$\times\left[h_xh_y\left(\frac{1}{h_y}\frac{\partial\bar{v}_x}{\partial z}+\frac{1}{h_x}\frac{\partial\bar{v}_y}{\partial z}+\frac{1}{h_y}\frac{\partial\bar{v}_z}{\partial x}+\frac{1}{h_x}\frac{\partial\bar{v}_z}{\partial y}\right)\right]$$
$$+\epsilon h_x\frac{\partial}{\partial z}\left(\frac{\partial\bar{v}_x}{\partial x}+\frac{\partial\bar{v}_y}{\partial y}\right)-\epsilon^2h_xh_y\frac{\partial}{\partial y}\left(\frac{\partial\bar{v}_x}{\partial x}+\frac{\partial\bar{v}_y}{\partial y}\right)$$
$$-\epsilon^2\frac{\partial}{\partial x}\left[h_x^2h_y^2\left(\frac{1}{h_y^2}\frac{\partial\bar{v}_x}{\partial x}+\frac{1}{h_xh_y}\frac{\partial\bar{v}_x}{\partial y}\right.\right.$$
$$\left.\left.+\frac{1}{h_x^2}\frac{\partial\bar{v}_y}{\partial y}+\frac{1}{h_xh_y}\frac{\partial\bar{v}_y}{\partial x}-\left(\frac{1}{h_x^2}+\frac{1}{h_y^2}\right)\frac{\partial\bar{v}_z}{\partial z}\right)\right]\Bigg\}$$
$$+i_y\left\{(1-\epsilon^2h_y^2)\frac{\partial}{\partial y}\left(\frac{\partial\bar{v}_x}{\partial x}+\frac{\partial\bar{v}_y}{\partial y}\right)+\left(\epsilon\frac{\partial}{\partial y}+\epsilon^2h_y\frac{\partial}{\partial z}\right)\right.$$
$$\times\left[h_xh_y\left(\frac{1}{h_y}\frac{\partial\bar{v}_x}{\partial z}+\frac{1}{h_x}\frac{\partial\bar{v}_y}{\partial z}+\frac{1}{h_y}\frac{\partial\bar{v}_z}{\partial x}+\frac{1}{h_x}\frac{\partial\bar{v}_z}{\partial y}\right)\right]$$
$$+\epsilon h_y\frac{\partial}{\partial z}\left(\frac{\partial\bar{v}_x}{\partial x}+\frac{\partial\bar{v}_y}{\partial y}\right)-\epsilon^2h_xh_y\frac{\partial}{\partial x}\left(\frac{\partial\bar{v}_x}{\partial x}+\frac{\partial\bar{v}_y}{\partial y}\right)$$
$$-\epsilon^2\frac{\partial}{\partial y}\left[h_x^2h_y^2\left(\frac{1}{h_y^2}\frac{\partial\bar{v}_x}{\partial x}+\frac{1}{h_xh_y}\frac{\partial\bar{v}_x}{\partial y}\right.\right.$$
$$\left.\left.+\frac{1}{h_x^2}\frac{\partial\bar{v}_y}{\partial y}+\frac{1}{h_xh_y}\frac{\partial\bar{v}_y}{\partial x}-\left(\frac{1}{h_x^2}+\frac{1}{h_y^2}\right)\frac{\partial\bar{v}_z}{\partial z}\right)\right]\Bigg\}$$
$$+i_z\left\{\left[\epsilon h_x\frac{\partial}{\partial x}+\epsilon h_y\frac{\partial}{\partial y}+\epsilon^2(h_x^2+h_y^2)\frac{\partial}{\partial z}\right]\left(\frac{\partial\bar{v}_x}{\partial x}+\frac{\partial\bar{v}_y}{\partial y}\right)\right.$$
$$+\left(\epsilon^2h_x\frac{\partial}{\partial x}+\epsilon^2h_y\frac{\partial}{\partial y}\right)$$
$$\left.\times\left[h_xh_y\left(\frac{1}{h_y}\frac{\partial\bar{v}_x}{\partial z}+\frac{1}{h_x}\frac{\partial\bar{v}_y}{\partial z}+\frac{1}{h_y}\frac{\partial\bar{v}_z}{\partial x}+\frac{1}{h_x}\frac{\partial\bar{v}_z}{\partial y}\right)\right]\right\}+O(\epsilon^3). \tag{B 8}$$

Finally, use

$$\boldsymbol{\varepsilon}:\nabla_s\bar{v}=-\bar{\nabla}_s\times\bar{v}, \tag{B 9}$$

where

$$\boldsymbol{\varepsilon}=i_x(i_yi_z-i_zi_y)+i_y(i_zi_x-i_xi_z)+i_z(i_xi_y-i_yi_x) \tag{B 10}$$

is the unit alternator triadic, to find

$$(\nabla_s \times \bar{v})\cdot \boldsymbol{n} = \frac{\partial \bar{v}_y}{\partial x} - \frac{\partial \bar{v}_x}{\partial y} + \epsilon\left[h_y\left(\frac{\partial \bar{v}_z}{\partial x} - \frac{\partial \bar{v}_x}{\partial z}\right) + h_x\left(\frac{\partial \bar{v}_y}{\partial z} - \frac{\partial \bar{v}_z}{\partial y}\right)\right] + \tfrac{1}{2}\epsilon^2(h_x^2 + h_y^2)\left(\frac{\partial \bar{v}_x}{\partial y} - \frac{\partial \bar{v}_y}{\partial x}\right) + O(\epsilon^3). \quad \text{(B 11)}$$

The equations of this Appendix may be employed to express (2.50) in explicit component form to $O(\epsilon^3)$.

REFERENCES

ARIS, R. 1962 *Vectors, Tensors and the Basic Equations of Fluid Mechanics.* Prentice Hall.

BOUSSINESQ, M. J. 1913 Sur l'existance d'une viscosité superficielle dans la mince couche de transition séparant un liquide d'une autre fluide contigu. *Ann. Chem. Phys.* **29**, 349–357.

BURELBACH, J. P., BANKOFF, S. G. & DAVIS, S. H. 1988 Nonlinear stability of evaporating/condensing liquid films. *J. Fluid Mech.* **195**, 463–472.

DERYAGUIN, B. V. 1955 Definition of the concept of and magnitude of the disjoining pressure and its role in the statics and kinetics of thin layers of liquids. *Colloid J. USSR* **17**, 191–197.

DERYAGUIN, B. V. & KUSAKOV, M. M. 1937 Experimental study of solvation of surfaces as applied to the mathematical theory of the stability of lyophilic colloids. *Akad. Nauk. SSSR, Khim.* **6**, 1119–1152.

DERYAGUIN, B. V. & LANDAU, L. 1941 Theory of the stability of strongly charged lyophobic sols and of the adhesion of strongly charged particles in solutions of electrolytes. *Acta Physicochim. (USSR)* **14**, 633–662.

EDWARDS, D. A., BRENNER, H. & WASAN, D. T. 1991 *Interfacial Transport Processes and Rheology.* Butterworth-Heineman.

FELDERHOF, B. U. 1968 Dynamics of free liquid films. *J. Chem. Phys.* **49**, 44–68.

GENNES, P. G. DE, HUA, L. & LEVINSON, P. 1990 Dynamics of wetting: local contact angles. *J. Fluid Mech.* **212**, 55–63.

JAIN, R. K. & RUCKENSTEIN, E. 1976 Stability of stagnant viscous films on a solid surface. *J. Colloid Interface Sci.* **54**, 108–116.

JENSEN, O. E. & GROTBERG, J. B. 1992 Insoluble surfactant spreading on a thin viscous film: shock evolution and rupture. *J. Fluid Mech.* **240**, 259–288.

LUCASSEN, J. & HANSEN, R. S. 1966 Damping of waves on monolayer covered surfaces. I. Systems with negligible surface dilatational viscosity. *J. Colloid Interface Sci.* **22**, 32–44.

MALDARELLI, C. & JAIN, R. K. 1982 The linear, hydrodynamic stability of an interfacially perturbed, transversely isotropic, thin, planar viscoelastic film. I. General formulation and a derivation of the dispersion equation. *J. Colloid Interface Sci.* **90**, 233–261.

MALDARELLI, C., JAIN, R. K., IVANOV, I. & RUCKENSTEIN, E. 1980 Stability of symmetric and unsymmetric thin liquid films to short and long wavelength perturbations. *J. Colloid Interface Sci.* **78**, 118–143.

ORON, A. & EDWARDS, D. A. 1993 Stability of a falling film in the presence of interfacial viscous stress. *Phys. Fluids* A **5**, 506–508.

PRIEVE, D. C. & RUSSEL, W. B. 1988 Simplified predictions of Hamaker constants from Lifshitz theory. *J. Colloid Interface Sci.* **125**, 1–13.

RUCKENSTEIN, E. & JAIN, R. K. 1974 Spontaneous rupture of thin liquid films. *Chem. Soc. Faraday Trans.* **270**, 132–137.

SALAMON, T. R., ARMSTRONG, R. C. & BROWN, R. A. 1994 Traveling waves on vertical films: Numerical analysis using the finite element method. *Phys. Fluids* A **6**, 2202–2220.

SCHE, S. & FIJNAUT, H. M. 1978 Dynamics of thin free liquid films stabilized with ionic surfactants. *Surface Sci.* **76**, 186–202.

SHARMA, A. & RUCKENSTEIN, E. 1986 An analytical nonlinear theory of thin film rupture and its application to wetting films. *J. Colloid Interface Sci.* **113**, 456–479.

SHAW, D. J. 1980 *Introduction to Colloid and Surface Chemistry.* Butterworths.

SILVEY, A. 1916 The fall of mercury droplets in a viscous medium. *Phys. Rev.* **7**, 106–111.

TAN, M. J., BANKOFF, S. G. & DAVIS, S. H. 1990 Steady thermocapillary flows of thin liquid layers. I. Theory. *Phys. Fluids* A **2**, 313–320.

TING, L., WASAN, D. T. & MIYANO, K. 1985 Longitudinal surface waves for the study of dynamic properties of surfactant systems II. Liquid–liquid interface. *J. Colloid Interface Sci.* **107**, 345–354.

TING, L., WASAN, D. T., MIYANO, K. & XU, S. Q. 1984 Longitudinal surface waves for the study of dynamic properties of surfactant systems I. Gas–liquid interface. *J. Colloid Interface Sci.* **102**, 248–253.

VERWEY, E. J. W. & OVERBEEK, J. T. G. 1948 *Theory of the Stability of Lyophobic Colloids*. Elsevier.

WHITAKER, S. 1964 Effect of surface active agents on the stability of falling liquid films. *Indust. Engng Chem. Fundam.* **3**, 132–142.

WILLIAMS, M. B. & DAVIS, S. H. 1982 Nonlinear theory of film rupture. *J. Colloid Interface Sci.* **90**, 220–232.